

Anomalous First Order Transition in $Nd_{0.5}Sr_{0.5}MnO_3$: An interplay between kinetic arrest and thermodynamic transitions

R. Rawat, K. Mukherjee, Kranti Kumar, A. Banerjee and P. Chaddah*

UGC-DAE Consortium for Scientific Research

University Campus, Khandwa Road

Indore-452017, M.P, India.

(Dated: December 2, 2024)

A detailed investigation of the first order antiferromagnetic insulator to ferromagnetic metal transition in $Nd_{0.5}Sr_{0.5}MnO_3$ is carried out by resistivity and magnetization measurements. These studies reveal several anomalous features that are explained as an outcome of hindered first order transition with glass like arrest of kinetics. We used a simple phenomenological model, which considers the interplay of kinetic arrest and thermodynamic transitions. Based on this model a H-T phase diagram is proposed which consists of kinetic arrest band and supercooling and superheating spinodal. Using this phase diagram observed state of the system can be predicted for any path in H-T space, unambiguously. This model is verified with magnetic field annealing measurements which also show that regions having higher kinetic arrest temperature have lower supercooling temperature, and vice versa.

PACS numbers: 75.47.Lx, 75.30.Kz

I. INTRODUCTION

The compound $Nd_{0.5}Sr_{0.5}MnO_3$ (NSMO) undergoes a paramagnetic insulator (PMI) to ferromagnetic metal (FMM) transition around $T_C \approx 255K$ and FMM to antiferromagnetic insulator (AFI) transition at low temperature $T_N \approx 150K^{1,2}$. The PMI to FMM transition, which is a generic feature of hole doped perovskite manganites, is second order in nature and shifts to higher temperature with the application of magnetic field. Whereas, the FMM to AFI transition is first order, which is accompanied by hysteretic resistivity across the transition. Below T_N system can be driven from AFI to FMM state with the application of magnetic field and shows open hysteresis loop in field dependence of resistivity (RH)^{1,2}. Such anomalous behavior in this compound and analogous systems were considered to be arising from supercooling at low temperatures where thermal fluctuations are suppressed^{1,2,3}. However, there remains many unexplained features which can not be answered using supercooling alone. In fact, Manekar et al⁴, from their studies on the system $Ce(Fe_{0.96}Al_{0.04})_2$, had suggested the role of kinetic arrest in NSMO also. According to their phenomenological model, below a certain temperature, called kinetic arrest temperature (T_K), the transformation from high temperature to low temperature phase is hindered on laboratory time scale due to critically slow dynamics of phase transformation. Such arrested phase has been shown in several intermetallic systems and $La - Pr - Ca - Mn - O$, where this model successfully explained the observed anomalies^{5,6,7,8}.

In this paper we present a systematic investigation of first order transition in NSMO, using resistivity and magnetization measurements. Our study not only clarify previously observed anomalous behavior in resistivity but also bring to light new observations. These lead to a phase diagram consistent with that suggested by

Manekar et al.⁴

II. EXPERIMENTAL DETAILS

The polycrystalline NSMO is prepared by solid state reaction method and characterized by powder x-ray diffraction. Reitveld analysis of x-ray diffraction data and iodometric titration shows that compound is single phase and stoichiometric. Resistivity measurements are performed by standard four probe technique using a commercial cryostat (Oxford Instruments Inc., UK) with 8-Tesla magnetic field. Magnetization measurements are carried out using a commercial 14 Tesla Vibrating Sample Magnetometer (Quantum Design, PPMS-VSM).

III. RESULTS AND DISCUSSION

Figures 1(a) and (b), respectively, show the temperature dependence of the resistivity in the absence of magnetic field and magnetization in the presence of 500 Oe magnetic field during cooling and heating for the compound NSMO. Both the measurements shows two transitions. The high temperature transition from paramagnetic insulator (PMI) to ferromagnetic metallic (FMM) phase is indicated by a sharp increase in magnetization around 230 K and changeover from insulator like to metal like behaviour in resistivity around 200 K. At low temperatures a sharp rise in resistivity around 120 K and corresponding decrease in magnetization with decreasing temperature, indicates another transition from FMM to antiferromagnetic insulating (AFI) phase. Transition from FMM to AFI phase is accompanied by a large thermal hysteresis which indicates first order nature of this transition. As can be seen from Figure 1, the transitions during cooling as well as warming, both are quite

broad ($\Delta T \approx 50K$). The broad transition can be associated with disorder which is natural to multicomponent systems. It results in different supercooling (T^*) and superheating (T^{**}) temperature for different regions of the samples⁹. Therefore for a macroscopic system it results in a band of supercooling (T^*) and superheating (T^{**}) temperature. Present observations on our polycrystalline NSMO are in qualitative agreement with studies on single crystalline NSMO by Kuwahara et al.¹ and Tokura et al.² They^{1,2} also observed a second order PMI to FMM transition at higher temperatures followed by a first order FMM to AFI transition at low temperature. The quantitative difference like relatively smaller change in resistivity could be due to disorder inherent in polycrystalline samples. However, these differences between the two samples are unimportant for the present discussion and conclusions drawn in this manuscript will be applicable to both kind of systems.

Figure 2 shows the magnetic field dependence of the resistivity (RH) and magnetization (MH) at various constant temperatures. For these isothermal measurements sample is cooled under zero field and then magnetic field is applied to measure the field dependence of resistivity and magnetization. With increasing magnetic field (path i: $0 \rightarrow H_{max}$) both resistivity and magnetization shows magnetic field induced transition from AFI to FMM phase. As can be seen from figure 2, the magnetic field required for this transition (H_{up}) decreases with increasing temperature. With decreasing field (path ii: $H_{max} \rightarrow 0$) the reverse transition from FMM to AFI as seen in Figure 2(b), (c), (e), (f) starts at lower field compared to H_{up} . The magnetic field required for FMM to AFI transition (H_{dn}) decreases with decreasing temperature at low temperatures and at 5K [Figure 2(a) and (d)] there is no clear signature of FMM to AFI transformation. Besides this at low temperatures FMM to AFI transformation does not complete even up to zero magnetic field which is clearly visible in RH data shown in Figure 2(a) and (b). There is a large difference between two values of zero field resistivity that is before and after application of magnetic field, giving rise to open hysteresis loop. As can be seen from figure 2(b) and (c), the difference between two values of zero field resistivity decreases with increasing temperature. The observed field induced transition and open hysteresis loop are in agreement with the magnetoresistance studies on single crystalline NSMO^{1,2}.

To study the magnetic state after path ii, we complete the envelop curve. The envelope curve is obtained from field cycling from $0 \rightarrow -H_{max} \rightarrow 0 \rightarrow +H_{max}$ and again $+H_{max} \rightarrow 0$ (path: iii-v). Both resistivity and magnetization show a butterfly like shape. An anomalous feature which is prominent in both RH and MH curves at low temperature is that the virgin curves (path i: $0 \rightarrow H_{max}$) stay outside the envelop curves (path iii to v: $0 \rightarrow -H_{max} \rightarrow +H_{max}$). This striking anomaly does not show up in RH or MH measurements if only the paths (i) and (ii) are traversed. This is evident in the study of

RH for NSMO¹ and the studies of RH as well as MH in analogous systems $(Nd_{1-y}Sm_y)_{1/2}Sr_{1/2}MnO_3$ ^{2,3}. Thus the anomaly in the field induced first order process is clearly brought out pursuing paths iii-v for RH or MH. It is to be noted that the difference between the virgin and forward envelop curve decreases with increasing temperature.

To show that these anomalous features are not related to spin glasses, superparamagnets or domain wall dynamics in ferromagnets, resistivity and magnetization measurements in presence of 1 and 2 Tesla magnetic field were performed as shown in Fig. 3. For these measurements the sample is cooled under zero field condition to the lowest temperature of measurement and then resistivity and magnetization is measured under above mentioned constant magnetic field in following sequence: (a) warming to highest temperature of measurement (ZFC), (b) cooling under same field to lowest temperature (FCC) and again (c) warming under same field (FCW). As can be seen from Figure 3 (a), with the increase in magnetic field the FCC and FCW curve shows a reduction in transition temperature. These observations are consistent with the resistivity measurement on single crystalline NSMO^{1,2}. However, ZFC curves, which were not shown earlier for NSMO, show anomalous behavior. At low temperature there is a large difference between ZFC and corresponding FC (field cooled) curves. Similar behavior is observed in magnetization measurements (Fig. 3(b)), which shows distinctly higher magnetization for FCW/FCC curve compared to ZFC below transition temperature. Though such bifurcation in the history dependent magnetization is expected to arise for metastable magnetic systems or domain wall dynamics in ferromagnets, contrary to present observations (Fig. 3), it is generally not coupled with similar bifurcation in resistivity. Moreover, the increase in the difference between the ZFC and FC curves with increasing magnetic field does not take place for any of the above mentioned systems contrary to the observation in fig. 3(b). For all such conventional systems the bifurcation between ZFC and FC magnetization actually decreases with the increase in field.

Fig. 4(a) shows the H-T phase diagram for first order transformation in NSMO, which is obtained from isothermal MH and RH curves. This phase diagram shows the temperature dependence of H_{up} (critical field required for AFM to FMM transition) and H_{dn} (critical field required for FMM to AFM transition). These values of magnetic field are obtained from the isothermal MH and RH curve recorded at several temperatures and critical field values are taken as the magnetic field at which first derivative of magnetization in MH and second derivative of resistivity in RH shows an extremum. Due to absence of sharp features in RH curves across the transition, calculated critical field can have larger error compared to that obtained from MH curves. This phase diagram shown in fig. 4(a) is qualitatively similar to phase diagram of single crystalline NSMO^{1,2}. As expected, H_{up} increases with decreasing

temperature. Whereas H_{dn} initially increases with decreasing temperature shows a shallow maxima around 60 K (T_a) and then starts decreasing with further lowering temperature. Such anomalous feature is more obvious in MH curves recorded at different temperatures as shown in Figure 5 (a) and (b). As can be observed from Figure 5(a) and (b) the forward MH curve ($0 \rightarrow H_{max}$) moves monotonically to lower field values with increasing temperature from 5 to 100 K. Whereas, the return MH curve ($H_{max} \rightarrow 0$) moves to higher field values with increasing temperature below 60 K [Figure 5(a)] and then moves to lower field values above 60K [Figure 5(b)].

From these observations it is obvious that the observed anomalous behavior in NSMO can not be explained as disorder broadened phase transformation only. Some of these anomalous behaviour which are observed for NSMO, has also been observed in other system e.g. $Ce(Fe_{0.96}Al_{0.04})_2$ ^{4,10} and Pr doped $La_{5/8}Ca_{3/8}MnO_3$ ^{11,12}. In these studies it is attributed to blocked metastable phase coexisting with stable phase at low temperatures. In case of $Ce(Fe_{0.96}Al_{0.04})_2$ ^{4,10} it has been shown that due to critically slow dynamics of phase transition, the transformation from high temperature to low temperature phase is hindered on laboratory time scale resulting in a blocked metastable (or glass like) states at low temperatures. It is worth to note here that such metastable kinetically arrested (or glass) states are different from the metastable supercooled state^{8,13}. It has been already highlighted in Kranti Kumar et al.⁸ that *such metastable kinetically arrested (or glass) state is different from metastable supercooled state in that the latter (but not the former) will undergo metastable to stable transformation on lowering temperature. In other words relaxation time decreases with decrease in temperature for supercooled state whereas the relaxation time increases with decrease in temperature for glassy state.*

From the above mentioned arguments it is evident that one needs to consider the role of kinetic arrest to explain the anomalous behavior in NSMO. Manekar et al.⁴ have also suggested that observed anomalous behavior in NSMO² could be explained using H-T phase diagram similar to their H-T phase diagram for $Ce(Fe_{0.96}Al_{0.04})_2$. Such schematic H-T diagram for NSMO, consisting of kinetic arrest band (H_K, T_K) and supercooling (H^*, T^*)and superheating spinodals (H^{**}, T^{**}), is shown in Fig 4(b). Using this diagram one can explain and predict the state of the system for different path in the H-T space and also verify its applicability for the given system. Let us consider path AB, which corresponds to Figure 1 (a), where sample is cooled under zero field condition from say 300-5K. For this path entire sample is transformed to AFI phase below (H^*, T^*) band as it is crossed before (H_K, T_K) band is reached. Therefore, at point B we have only AFI phase. When a magnetic field is applied under isothermal condition [Figure 2(a) and (d)], that is traversing B to E path in Figure 4 (b), it transform to FMM state on crossing (H^{**}, T^{**}) band. Both AFI and FMM phase co-exists within this band and for

magnetic fields higher than (H^{**}, T^{**}) only FMM phase exists. With reducing magnetic field in the absence of kinetic arrest, we expect reverse transformation to AFI phase will complete on crossing (H^*, T^*) band and result in AFI state for magnetic fields less than (H^*, T^*) band. However, due to (H_K, T_K) band FMM phase is arrested because the (H^*, T^*) band is at lower temperature compared to arrest band. Therefore the reverse transformation now can start only after crossing the (H_K, T_K) band in opposite sense while reducing the field (E to B path). Since, at this temperature, (H_K, T_K) band spreads to zero field values, only a fraction of FMM phase is transformed to AFI phase. It results in different zero field resistivity before (fully AFI) and after (AFI + FMM) the application of magnetic field. Since envelop curve for resistivity and magnetization starts from this point (traversing B to E and E to B path), it results in a much smaller resistivity and higher magnetization for envelop curve compared to virgin curve. Therefore virgin curve lies outside envelop curve. At higher temperatures more and more phase will get dearrested with reducing magnetic field resulting in smaller difference between virgin and envelope curve. This is shown in figure 2, where difference between virgin and envelop curve decreases for higher temperatures. For temperatures $T \geq T_a$, (H^*, T^*) will determine the FMM to AFI transition during isothermal measurements, as with decreasing magnetic field dearrest will take place before hitting the corresponding supercooling line for a particular region. It explains the anomalous behavior observed for the ZFC return transition curve in Figure 5 (a) and (b). The forward MH curve shifts monotonically to lower field values with increasing temperature because it depends on (H^{**}, T^{**}) band only which decreases monotonically to zero with increasing temperature. Whereas the return MH curve depends on (H_K, T_K) band below T_a as reverse transformation (FMM to AFI) takes place only after crossing this band. Since (H_K, T_K) band increases with increasing temperature, the return MH curve for $T \leq T_a$ shifts to higher field values with increasing temperature. Whereas, above T_a , FMM to AFI transformation takes place across (H^*, T^*) band, therefore return MH curve shifts to lower field values with further increase in temperature.

Now, consider the results of Figure 3, which were performed along path CD under different conditions. For ZFC curve, we reached the lowest temperature i.e. point C, along path AB (under zero field) and then applied magnetic field isothermally to reach point C. As explained above, sample will be in completely AFI state at point B and since point C is below (H^*, T^*) band, AFI state will persist at this point. Therefore ZFC run along path CD starts from point C with completely AFI phase. The transition to FMM phase will occur on crossing the (H^{**}, T^{**}) band. FCC curve will starts from point D with fully FMM phase and transformation to AFI phase will complete on crossing the (H^*, T^*) band. However, for some regions of the sample (H_K, T_K) lines will be crossed before the corresponding (H^*, T^*) lines⁸. There-

fore, there will be only a partial transformation from FMM to AFI phase and some regions will be arrested in FMM state. Since FMM phase is arrested and cannot transform to the equilibrium AFI phase on laboratory time scale, this coexistence will persist in field cooling down to the lowest temperature. This is in contrast to ZFC curve where at point C entire sample is in AFI state therefore having much higher resistivity or lower magnetization compared to FCC. Similarly, FCW curve will start with partial FMM phase and with warming dearrest will start on reaching (H_K, T_K) band and AFI phase will completely transform to FMM phase on crossing (H^{**}, T^{**}) band. If we increase the magnetic field to say 2 Tesla, then arrest band will appear at higher temperature resulting in more arrested FMM phase. Beyond certain field values entire sample will cross (H_K, T_K) band before crossing the (H^*, T^*) band during cooling (e.g. path GH) resulting in a completely arrested FMM phase at low temperature.

Kinetic arrest and dearrest can be demonstrated, more explicitly, by field annealing measurements¹³. For these measurements a constant magnetic field H_{an} (annealing field) is applied above (H^*, T^*) and (H_K, T_K) band and then sample is cooled to selected temperatures to record isothermal RH or MH curve with reducing field from H_{an} to zero. Results of such measurement are shown in Fig 6. As shown in Figure 6(a) resistivity values are dependent on annealing fields H_{an} in which sample is cooled to 5 K. The observed change in resistivity with reducing magnetic field at 5 K is much smaller compared to change in resistivity produced by different annealing field. It results in a large difference in resistivity values at $H=0$ for different annealing field. Smaller resistivity values with increasing H_{an} indicates larger fraction of arrested FMM phase. At 5 K only a small fraction of sample crosses the (H_K, T_K) band as magnetic field is reduced to zero. Therefore most of the arrested FMM phase remains arrested down to zero magnetic field. This is consistent with magnetization at 10K (Figure 6(d)) where magnetization depend on annealing field. For fields higher than 3 Tesla magnetization has negligible field dependence on H_{an} and it is around $3\mu_B/\text{Mn}$. From a comparison with saturation magnetization at 10 K we infer almost fully ferromagnetic phase for annealing field larger than 3 Tesla. For annealing field 2 and 1 Tesla magnetization is equivalent to $\approx 80\%$ and 30% FMM phase, respectively. At 25 K with reducing magnetic field sample crosses the (H_K, T_K) band at higher field value therefore a larger fraction of sample get dearrested to AFI phase. It is evident from RH and MH curves at 25K, where we observe a sharp increase in resistivity with lowering magnetic field for $H_{an} = 2$ and 3 Tesla and both the curve merges around ≈ 0.5 Tesla indicated by vertical arrow in the figure 6(b) and (e). Whereas 1 Tesla resistivity remains higher for all the field values down to 0 Tesla. It suggests that regions which are arrested for

field $H_{an} \geq 2$ Tesla are dearrested at 25 K with reducing magnetic field. At 40K, as shown in figure 6(c) and (f), all the curves (1,2 and 3 Tesla) merge together with decreasing magnetic field and merger point shifted to higher field values compared to 25 K, which indicates that regions which are arrested for field values $H_{an} \geq 1$ Tesla are dearrested with decreasing magnetic field. This observation shows that the regions which are arrested for higher annealing field values shows dearrest at $H=0$ at lower temperature^{8,13}. Therefore, the region arrested in higher annealing field lie to the high temperature end of the (H^*, T^*) band, but dearrest at higher H on isothermal reduction of field indicates such regions lie to the low temperature end of the (H_K, T_K) band. The behavior of our MH curves [Figure 6(d)-(e)] is similar to corresponding studies on the compound $\text{Ce}(\text{Fe}_{0.98}\text{Os}_{0.02})_2$ ⁸, which also shows a first order FM to AFM transition with lowering temperature and kinetically arrested ferromagnetic phase. From these studies we infer that (H_K, T_K) band and (H^*, T^*) band are anticorrelated in NSMO⁸ i.e. regions which have higher (H_K, T_K) have lower (H^*, T^*) .

IV. CONCLUSIONS

Anomalous nature of first order AFI to FMM transition in NSMO has been elucidated by transport and magnetic measurements. It has been shown that one has to invoke glass like arrest of kinetics to explain observed thermo-magnetic irreversibility in this system. A H-T phase diagram consisting of kinetic arrest band and supercooling and superheating spinodal has been proposed for this system. It has been shown that below 60 K, kinetic arrest dominates the FMM to AFI transition. This results in phase coexistence down to the lowest temperature when the sample is cooled in fields ranging from about 1 Tesla to 2 Tesla even though the equilibrium phase is AFI. The proposed H-T diagram is tested by field annealing measurements. Besides asserting the proposed H-T diagram, field annealing measurements also indicate that regions arrested at higher temperature (H_K, T_K) have lower supercooling temperature (H^*, T^*) and vice versa. Since this model depends on few parameter and describes the state of a system for any path in H-T space, similar studies will be useful for several other such systems where blocked metastable states have been observed.

V. ACKNOWLEDGEMENTS

We would like to thank S.B. Roy (RRCAT, Indore) for fruitful discussions. DST, Government of India is acknowledged for funding the VSM. KM acknowledges CSIR, India.

* On deputation from RRCAT, Indore

¹ H. Kuwahara, Y. Tomioka, A. Asamitsu, Y. Moritomo and Y. Tokura, *Science* **270**, 961 (1995)

² Y. Tokura, H. Kuwahara, Y. Moritomo, Y. Tomioka and A. Asamitsu, *Phys. Rev. Lett* **76**, 3184 (1996).

³ H. Kuwahara, Y. Moritomo, Y. Tomioka, A. Asamitsu, M. Kasai, R. Kumai and Y. Tokura, *Phys. Rev. B* **56**, 9386 (1997).

⁴ M.A. Manekar, S. Chaudhary, M.K. Chattopadhyay, K.J. Singh, S.B. Roy and P. Chaddah, *Phys. Rev. B* **64**, 104416 (2001).

⁵ C. Magen, L. Morellon, P. A. Algarabel, C. Marquina and M.R. Ibarra, *J. Phys. Condens. Matter* **15**, 2389 (2003).

⁶ M.K. Chattopadhyay, M.A. Manekar, A.O. Pecharsky, V.K. Pecharsky, K.A. Gschneidner, Jr. J. Moore, G.K. Perkins, Y.V. Bugoslavsky, S.B. Roy, P. Chaddah and L.F. Cohen, *Phys. Rev. B* **70**, 214421 (2004)

⁷ Kausik Sengupta and E.V. Sampathkumaran, *Phys. Rev. B* **73**, 020406(R) (2006).

⁸ Kranti Kumar, A.K. Pramanik, A. Banerjee, P. Chaddah, S.B. Roy, S. Park, C.L. Zhang and S.-W. Cheong, *Phys. Rev. B* **73**, 184435 (2006).

⁹ Y. Imry and M. Wortis, *Phys. Rev. B* **19**, 3580 (1979).

¹⁰ K.J. Singh, S. Chaudhary, M.K. Manekar, S.B. Roy and P. Chaddah, *Phys. Rev. B* **65**, 094419 (2002).

¹¹ L. Ghivelder and F. Parisi, *Phys. Rev. B* **71**, 184425 (2005).

¹² P.A. Sharma, Sung Baek Kim, T.Y. Koo, S. Guha and S-W. Cheong, *Phys. Rev. B* **71**, 224416 (2005).

¹³ P. Chaddah, A. Banerjee and S.B. Roy, cond-mat 0601095.

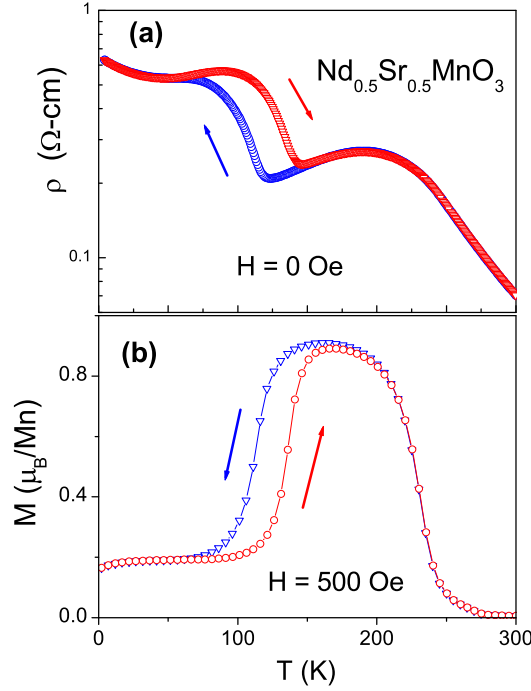


FIG. 1: (Color online) Temperature dependence of (a) resistivity in the absence of magnetic field and (b) magnetization in the presence of 500 Oe magnetic field for the compound $Nd_{0.5}Sr_{0.5}MnO_3$ during cooling and warming runs.

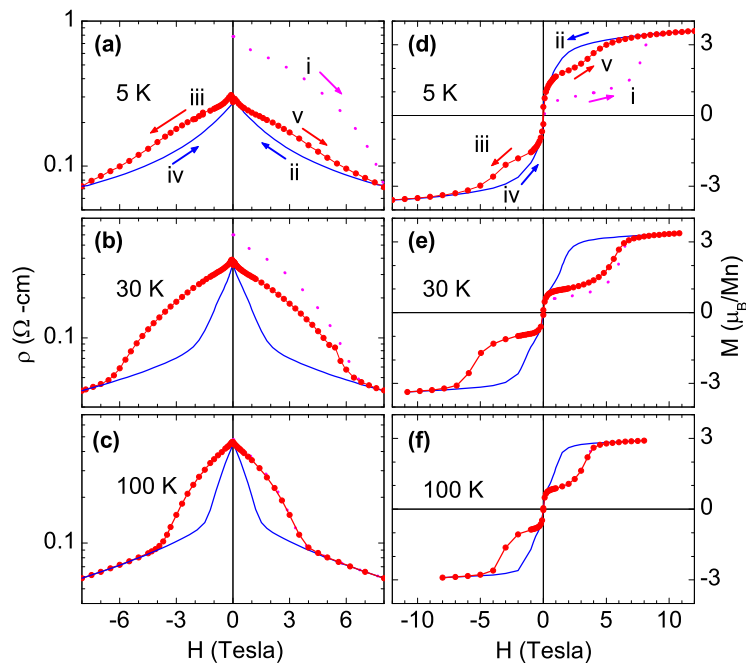


FIG. 2: (Color online) Magnetic field dependence of resistivity and magnetization at various constant temperatures for $Nd_{0.5}Sr_{0.5}MnO_3$. A large difference between zero field resistivity before and after the application of magnetic field is observed at low temperatures. Also both RH and MH curves show that virgin curve (dashed line) is lying outside the envelop curves.

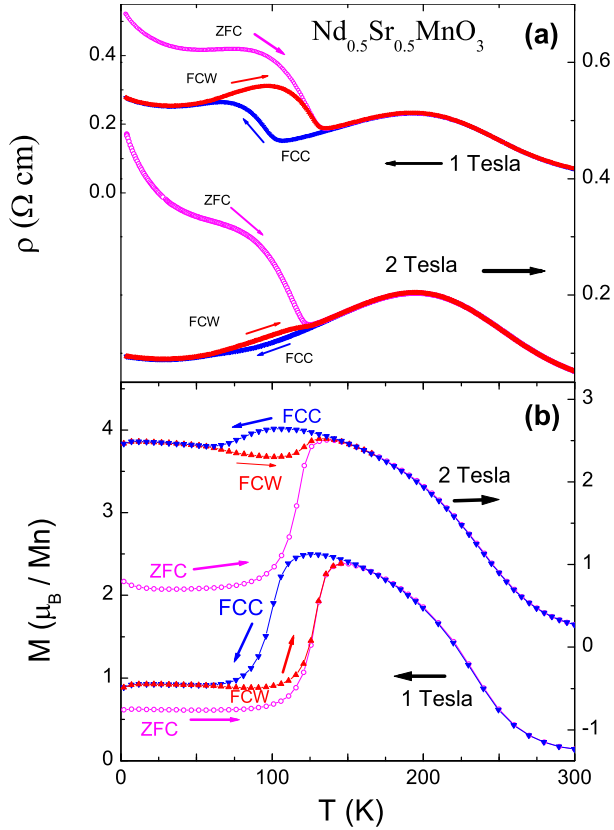


FIG. 3: (Color online) Temperature dependence of (a) resistivity and (b) magnetization for $Nd_{0.5}Sr_{0.5}MnO_3$ in presence of 1 and 2 Tesla magnetic field which is measured under different protocols. ZFC indicates measurement taken in the presence of applied magnetic field during warming for a zero field cooled sample, FCC/FCW indicates measurement taken during cooling/warming on a field cooled sample. Large difference between ZFC and FCC/FCW is clearly visible in all the measurements.

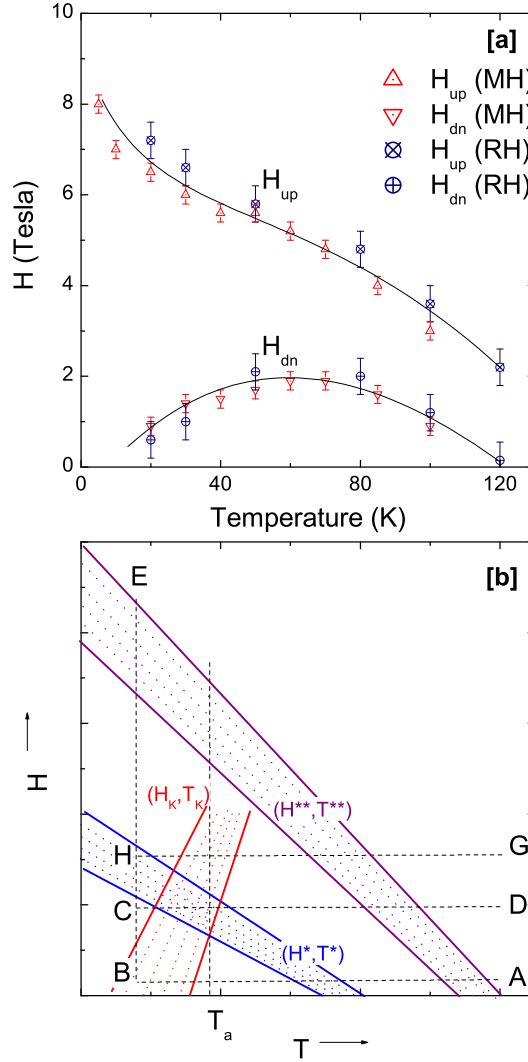


FIG. 4: (Color online) (a) H-T diagram of first order transition in the compound $Nd_{0.5}Sr_{0.5}MnO_3$, showing critical field required for AFI to FMM transitions (H_{up}) and FMM to AFI transition (H_{dn}). Triangles and circles, respectively represent the critical field obtained from isothermal M vs. H curve and R vs. H curves. Vertical line across the symbol are error bars. (b) Schematic representation of kinetic arrest (H_K, T_K) band, supercooling (H^*, T^*) and superheating (H^{**}, T^{**}) spinodals in H-T space for the compound $Nd_{0.5}Sr_{0.5}MnO_3$.

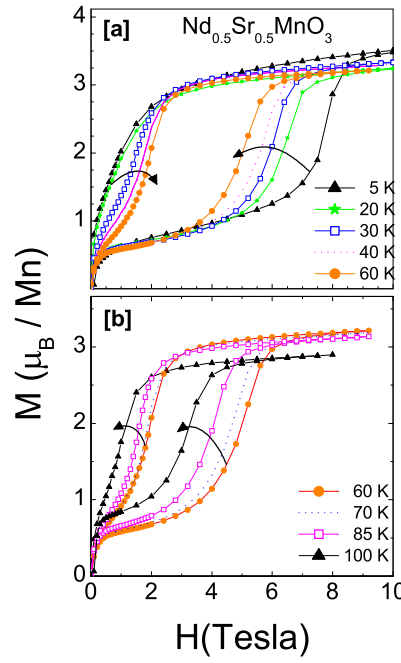


FIG. 5: (Color online) The magnetic field dependence of magnetization in $Nd_{0.5}Sr_{0.5}MnO_3$ at various temperatures showing return MH curve move (a) to higher field values below 60K and (b) to lower field values above 60K. The forward MH curve moves to lower field values monotonically with increasing temperature for all temperatures.

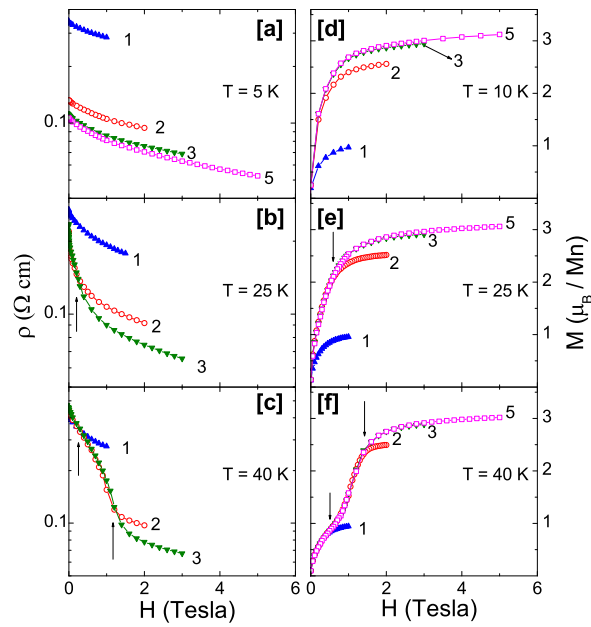


FIG. 6: (Color online) (a)-(c) RH and (d)-(f) MH at various constant temperatures for $Nd_{0.5}Sr_{0.5}MnO_3$ cooled under different annealing field H_{an} . Vertical arrows indicate dearrest field which is shifting to higher magnetic field with increasing temperature.